Journal of Applied Physics ARTICLE scitation.org/journal/jap

Structure and energy of the $\langle 1\bar{1}0\rangle$ screw dislocation in silicon using generalized Peierls theory

Cite as: J. Appl. Phys. **125**, 145702 (2019); doi: 10.1063/1.5083162
Submitted: 28 November 2018 · Accepted: 12 March 2019 ·
Published Online: 8 April 2019

View Online Export Citation CrossMark

Lili Huang and Shaofeng Wang[a)]

AFFILIATIONS

Department of Physics and Institute for Structure and Function, Chongqing University, Chongqing 401331, People's Republic of China

[a)]**E-mail:** sfwang@cqu.edu.cn

ABSTRACT

For the $\langle 1\bar{1}0\rangle$ screw dislocation (nondissociated) in silicon, there are three types of core structures that are, respectively, referred to as the shuffle-set dislocation (A-core), glide-set dislocation (C-core), and mix-set dislocation (B-core). Each type of core further displays a planar or nonplanar (fourfold) configuration. In this paper, in the context of the generalized Peierls theory, the energy functional and equation of equilibrium of a screw dislocation with a nonorthogonal fourfold structure is derived and is used to investigate the structure and energy of the $\langle 1\bar{1}0\rangle$ screw dislocation in silicon. We find that the energy of the shuffle-set dislocation with a fourfold core is considerably lower than that of the other types of cores. Thus, the shuffle-set dislocation with the fourfold core is the most stable. The glide-set dislocation with a planar core has the highest energy and is the most unstable. As the most stable structure, the shuffle-set screw dislocation with the fourfold core was responsible for wavy slip traces observed at low temperature.

I. INTRODUCTION

Although dislocations in silicon have been studied comprehensively both theoretically and experimentally,[1–15] many issues remain unresolved. One of them is the dislocation transition between the shuffle-set and the glide-set. As is well known, silicon is structured as a diamond cubic lattice consisting of two interpenetrating, face-centered-cubic (FCC) lattices offset by $\frac{1}{4}\langle 111\rangle$. Due to the coexistence of two FCC sublattices, there are two sets of {111} planes. The closely spaced set is called the glide-set and the widely spaced one the shuffle-set. Thus, there are two slip systems in the diamond lattice. Dissociated glide-set dislocations and perfect shuffle-set dislocations are thought to control the plastic deformation of semiconductors in high and low temperature regimes, respectively.[2,14,16]

Transmission electron microscopy (TEM) has revealed that specimens deformed at high temperature contain a large number of dissociated partial dislocations[17] that can only exist on the glide-set plane. Nondissociated dislocations were recently observed in silicon following deformation at low temperature and under high pressure.[18] Because shuffle-set dislocations cannot dissociate into partials whereas glide-set dislocations can, nondissociated dislocations are usually assumed to be shuffle-set. A TEM micrograph can show perfect dislocations aligned along the $\langle 110\rangle$, $\langle 112\rangle$, and $\langle 123\rangle$ directions. The observation of wavy slip traces indicates that the observed dislocations cross-slipped frequently.

As shown in Fig. 1, there are three types of $\langle 1\bar{1}0\rangle$ screw dislocations in silicon, referred to as the shuffle-set dislocation, called A-core, glide-set dislocation, called C-core, and mix-set dislocation, called B-core. The problems of dislocation mobility, core structure stability, and core transformation have attracted considerable research attention in the past.[9,11,12,14,19–21] Arias and Joannopoulos generated the atomic configuration of the A-core using the bonding topology proposed by Hornstra and calculated the core energy.[19,20] Koizumi *et al.* studied the B-core and proposed a mechanism of transformation between glide-set and shuffle-set dislocations.[9] They calculated the core structures and their stability using the Stillinger–Weber potential for interatomic interaction. Pizzagalli *et al.* investigated the stability of different cores of the screw dislocation using a classical simulation and first-principles calculation.[11,12] Wang *et al.* showed that based on extensive tight-binding

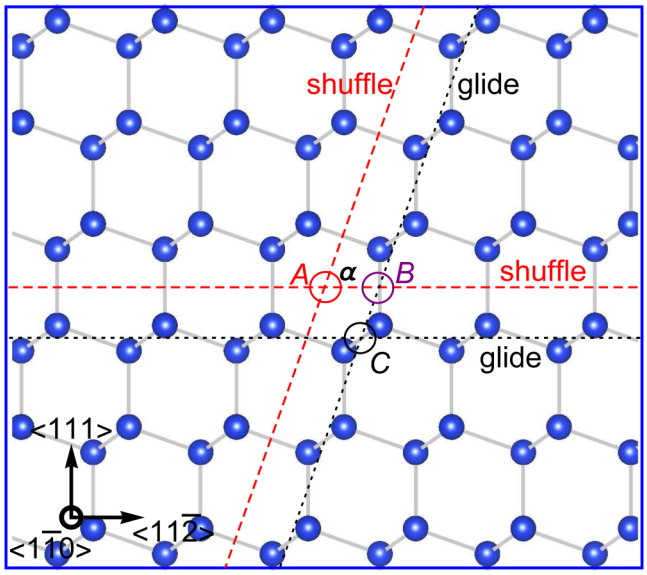

FIG. 1. Ball-and-stick representation of the $(1\bar{1}0)$ plane of the cubic diamond structure. The three circles A, B, and C indicate the positions of the cores of the dislocation, where the dislocation lines are perpendicular to the $(1\bar{1}0)$ plane. The dashed lines show shuffle-set dislocations, and the dotted lines show glide-set dislocations.

and density functional theory (DFT) calculations, the C-core of the screw dislocation has lower energy than that of the A-core following period-doubling reconstruction.[21] A theoretical study on the effects of pressure on the core properties of dislocations confirmed the stability of the reconstructed C-core.[13] The transformation of dislocation cores from the shuffle to the glide-set of {111} glide planes in Si was numerically examined by Li and Picu.[14] A mechanism leading to the formation of two 30° partial dislocations from the screw dislocation was discussed recently by Pizzagalli.[22] Miyata and Fujiwara studied the Peierls stress ($0.14\,\mathrm{eV/\AA^3} < \sigma_p < 0.19\,\mathrm{eV/\AA^3}$) of a straight screw dislocation in Si by an *ab initio* simulation of its molecular dynamics.[10] Pizzagalli and Beauchamp found that the Peierls stress is between $2.4 \times 10^{-2}\,\mathrm{eV/\AA^3}$ and $2.8 \times 10^{-2}\,\mathrm{eV/\AA^3}$ after considering the effects of the boundary conditions used in the first-principles calculation.[12] Joós *et al.* investigated shuffle-set screw dislocation using the Peierls–Nabarro model by combining generalized stacking fault energy, and the Peierls stress was estimated at $0.048\,\mathrm{eV/\AA^3}$.[23] Wang *et al.* calculated the Peierls stress, $\sigma_p \approx 0.8 \times 10^{-2}\,\mathrm{eV/\AA^3}$, using the Peierls–Nabarro (PN) model including discreteness correction.[24] The experimental results suggest that the Peierls stress is $0.043\,\mathrm{eV/\AA^3} < \sigma_p < 0.213\,\mathrm{eV/\AA^3}$.[25] Disagreement over the Peierls stress data was beyond the range of error.

While the $\langle 1\bar{1}0\rangle$ screw dislocation is classified into the A-, B-, and C-cores according to their centers, the equilibrium core structure is not uniquely determined when the center of a dislocation is given. Because a screw dislocation has many slip planes, the core structure of a screw dislocation may be planar or nonplanar[26] and may be further reconstructed. Therefore, the $\langle 1\bar{1}0\rangle$ screw dislocation may display a variety of core configurations. Furthermore, because the transition from a metastable core to a stable core is sometimes prevented owing to the local stability of covalent materials, it is important to clearly recognize the initial core structure in observations or the processes of evolution. Unfortunately, in experimental observations and numerical simulations, little work has emphasized multiple cores beyond distinct positions and revealed the precise core configuration. In this paper, multiple cores, including planar and nonplanar cores, and their stability are investigated for $\langle 1\bar{1}0\rangle$ screw dislocations in the frame of the generalized Peierls theory.[27,28] The energy functional and equilibrium equations for a screw dislocation with a nonorthogonal multifold core are successfully derived, and the structural stability of the $\langle 1\bar{1}0\rangle$ screw dislocation is studied in energetics. Our analytical results are helpful in understanding the properties of the $\langle 1\bar{1}0\rangle$ screw dislocation and the transition between the shuffle-set and the glide-set dislocations. In Sec. II, the γ-potential is calculated using the electron density function theory. In Sec. III, the energy functional and the dislocation equation are derived based on the concept of distribution of infinitesimal dislocations. In Sec. IV, the equilibrium core structures, stress field, and the difference displacement map are presented, and the energy of the structure is calculated. Section V contains a discussion and the summary of this paper.

II. γ-POTENTIAL OF {111} PLANE FOR PERFECT $\langle 1\bar{1}0\rangle$ SCREW DISLOCATION

While a small deformation in a solid is characterized by elastic constants, many phenomena in nonlinear mechanics are frequently characterized by generalized stacking fault (GSF) energy, which is also generally called the γ-surface.[29] In particular, the structure and properties of dislocations in materials are dominated by the γ-surface.[30–36] Although it is challenging to determine the γ-surface in experiments, it can be calculated in electron density functional theory, which has been widely used and proved to be reliable in predicting physical properties. To incorporate the spatial change induced by the dislocation, the γ-surface is generalized to the γ-potential including the change in the interaction energy with spatial variation.[8,37,38]

The γ-potential is defined as the interaction energy between parallel half-infinite crystals. When a crystal is cut into two half-infinite parts by a given cut plane parallel to a family of lattice planes, the interaction energy changes when the two parts undergo a relative rigid translation. The interaction energy per unit area as a function of the rigid translation is referred to as the γ-potential of the lattice plane. Because a rigid translation can be parallel or perpendicular to the cut plane, it is characterized by a three-dimensional (3D) vector $\mathbf{u}$. For a given γ-potential $\gamma(\mathbf{u})$, the force per unit area due to relative translation, $\mathbf{f} = (f_x, f_y, f_z)$, is given by the gradient of the γ-potential

$$\mathbf{f} = -\nabla\gamma(\mathbf{u}).$$

We are typically interested in the variation in the γ-potential along a high-symmetry direction, where it is given in a reduced way as a function of slip along the symmetrical direction. For the

$\langle 1\bar{1}0\rangle$ screw dislocation, only the γ-potential of the {111} plane along the $\langle 1\bar{1}0\rangle$ slip is involved. This γ-potential is calculated for silicon using the VASP package by using a slab consisting of 14 {111}-planes as the supercell. The generalized gradient approximation (GGA) as proposed by Perdew, Burke, and Ernzerhof (PBE) considers the exchange-correlation functional,[39,40] as well as the projector augmented wave (PAW) potentials.[41,42] It accounts for electron–ion interactions and is employed in all the DFT calculations. The thickness of the vertical vacuum was chosen as 10 Å, as usual. The plane-wave kinetic-energy cutoff is 500 eV, and the grid mesh is $15 \times 15 \times 1$. The calculated results for the γ-potentials of the shuffle-set and the glide-set dislocations are shown, respectively, in Figs. 2 and 3. Because of periodicity, the γ-potential can be well described by the following analytical expression:[43]

$$\gamma = \gamma_0 + \gamma_1 \cos^2\left(\frac{\pi u_s}{b}\right) + \gamma_2 \cos^4\left(\frac{\pi u_s}{b}\right), \tag{1}$$

where u_s is the relative displacement along the direction of slip and γ_i $(i = 0, 1, 2)$ is the function of the relative vertical displacement u_e (space change). γ_i $(i = 0, 1, 2)$ can be suitably expressed in terms of the Morse functions,

$$\gamma_0 = \phi_0, \quad \gamma_1 = -3\phi_0 - \phi_1 + 4\phi_2, \quad \gamma_2 = 2(\phi_0 + \phi_1 - 2\phi_2),$$

with

$$\phi_i(u_e) = \omega_i[e^{-3\eta_i\frac{(u_e - v_i)}{\tau}} - 2e^{-\frac{3}{2}\eta_i\frac{(u_e - v_i)}{\tau}}] + \varsigma_i,$$

where $\tau = 2.36$ Å is the bond length and ω_i, v_i, ς_i $(i = 0, 1, 2)$ are parameters listed in Table I.

III. ENERGY FUNCTIONAL AND DISLOCATION EQUATION FOR NONORTHOGONAL FOURFOLD CORE

Dislocation is a kind of topological defect characterized by the Burgers vector **b**, that is, the topological charge. Instead of a point-like defect, a single dislocation in a crystal possesses an extended structure, i.e., topology charge **b** is not concentrated at a point, but distributes in an extended manner. It is instructive to view a single dislocation as a condensate of infinitesimal dislocations. The concept of the condensate of infinitesimal dislocations was initially introduced by Eshelby, who recognized that the topology charge distribution of a dislocation is related to the gradient of the slip field. The concept was successfully used recently to study the non-planar screw dislocation in BCC crystals.[27,28] It was found that a screw dislocation has the tendency to spread the distribution on all possible slip planes.

As the condensate of infinitesimal dislocations, a perfect dislocation is characterized by the distribution of infinitesimal dislocations. The distribution of the screw dislocation is simply described by a scalar function $J_s(x, y)$, where the centerline of the screw dislocation is chosen as the z-axis,

$$\int\int J_s(x, y)dx\,dy = b.$$

As first proposed by Hirsch,[44] rather than a planar core structure, the core of a screw dislocation may distribute to several slip planes. While direct experimental observations of the cores of screw dislocations are difficult,[45–47] the concept of a multifold structure of the screw dislocation is widely accepted.[27,28,48–51]

For a screw dislocation with a multifold (n-fold) structure, the distributions $J_s(x, y)$ can be reduced to 1D distributions,[27]

$$J_s(x, y) = \sum_{\alpha=1}^{n} \rho_s^{\alpha}(x_\alpha)\delta(y_\alpha)\theta(x_\alpha), \tag{2}$$

with

$$x_\alpha = x\cos\phi_\alpha + y\sin\phi_\alpha, \quad y_\alpha = -x\sin\phi_\alpha + y\cos\phi_\alpha,$$

where ϕ_α is the angle between the α-th fold and the x-axis, $\rho_s^{\alpha}(x_\alpha)$ is the distribution of the infinitesimal screw along the α-th fold, and $0 \le x_\alpha \le \infty$ are the coordinates of the point on the fold. The distribution $\rho_s^{\alpha}(x_\alpha)$ is referred to as the fold distribution. For a symmetric multifold structure, the fold distribution is the same, $\rho_s^{\alpha}(x_\alpha) = \rho_s(x_\alpha)$, and we have

$$J_s(x, y) = \sum_{\alpha=1}^{n} \rho_s(x_\alpha)\delta(y_\alpha)\theta(x_\alpha). \tag{3}$$

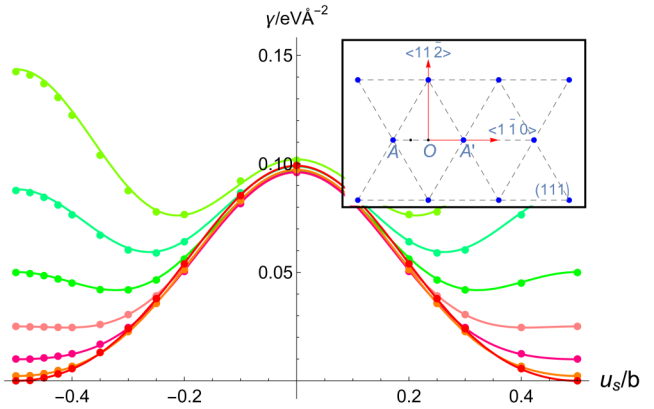

FIG. 2. γ-potential of shuffle-set in units of eV/Å^2. It is plotted as a function of the relative translation along the $\langle 1\bar{1}0\rangle$ direction for various spaces $d_s + u_e$, where d_s is the equilibrium space and u_e is the space change, $b = |AA'| = \sqrt{2}a_0/2$, and $a_0 = 5.46$ Å is the lattice constant. The solid lines are given by the analytical expression in Eq. (1) and the dotted lines by the first-principles calculations. For the shuffle-set dislocation, the space is narrowed when there is a dislocation, $u_e < 0$.

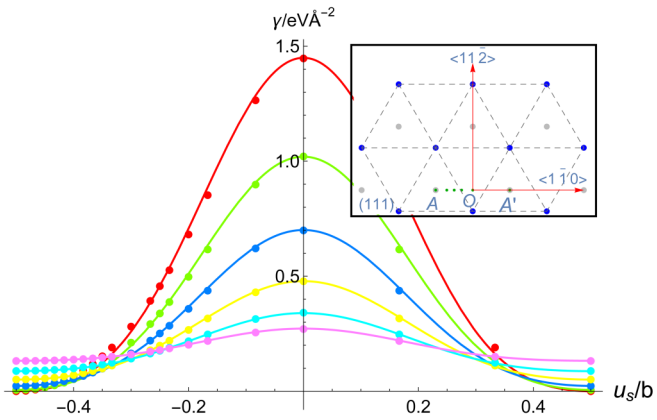

FIG. 3. γ-potential of glide-set as a function of the relative translation along the $\langle 1\bar{1}0\rangle$ direction for various space changes u_e. The solid lines are given by the analytical expression in Eq. (1) and the dotted lines by the first-principles calculations. For the glide-set dislocation, the space is broadened when there is a dislocation, $u_e > 0$.

An illustration of the nonorthogonal fourfold core structure of the $\frac{1}{2}\langle 1\bar{1}0\rangle$ screw dislocation is given in Fig. 4.

The interaction energy per unit length between parallel dislocation lines with the Burgers vectors $\mathbf{b}_1$ and $\mathbf{b}_2$ is given by[1]

$$\frac{W_{12}}{L} = -\frac{K_s}{2\pi}(\boldsymbol{b_1}\cdot\boldsymbol{\xi})(\boldsymbol{b_2}\cdot\boldsymbol{\xi})\ln\frac{R}{R_0} - \frac{K_e}{2\pi}[(\boldsymbol{b_1}\times\boldsymbol{\xi})\cdot(\boldsymbol{b_2}\times\boldsymbol{\xi})]\ln\frac{R}{R_0} - \frac{K_e}{2\pi R^2}[(\boldsymbol{b_1}\times\boldsymbol{\xi})\cdot\boldsymbol{R}][(\boldsymbol{b_2}\times\boldsymbol{\xi})\cdot\boldsymbol{R}], \quad (4)$$

where $\boldsymbol{\xi}$ is the unit vector along the dislocation line, $\mathbf{R}$ is the relative position vector of the two dislocation lines, $R = |\mathbf{R}|$ is distance, and K_s and K_e are energy factors. The first term in Eq. (4) describes the interaction between the screw components, and the last two terms in Eq. (4) describe the interaction between the edge components. From the principle of superposition, we know that for a symmetric core structure, the total interaction energy of infinitesimal screw dislocations can be written as

$$U_s = -\frac{K_s}{2\pi}\int_0^{+\infty}\int_0^{+\infty}\rho_s(x)\rho_s(x')\varphi_s(x,x')dx\,dx', \quad (5)$$

where, apart from a factor, $\varphi_s(x,x')$ can be interpreted as the effective interaction energy between unit screw dislocations located at x and x' in a fold. For a planar structure (twofold),[27]

$$\varphi_s(x,x') = \ln\frac{|x^2 - x'^2|}{R_0^2}. \quad (6)$$

For a nonorthogonal fourfold structure, it is found that (see the Appendix)

$$\varphi_s(x,x') = 2\ln\frac{|x^2 - x'^2|}{R_0^2} + \ln\frac{|x^4 + x'^4 - 2x^2x'^2\cos 2\alpha|}{R_0^4}, \quad (7)$$

where α is the angle between neighboring folds. If $\alpha = \pi/2$, the folds are perpendicular to each other, and the effective interaction equation (7) is the same as that given previously.[27]

When two neighboring lattice planes have a relative slip, the space changes to relax the energy. In particular, for the glide-set of silicon, the bonds connecting two glide planes are heavily compressed if the space is kept invariant. The existence of a screw dislocation implies a local relative slip, and it is then necessary to consider spatial variation induced by the dislocation. In this case, the spatial variation can be suitably viewed as the appearance of infinitesimal edge dislocations.[37] In an analogy to the screw dislocation, we introduce edge component distribution $J_e(x,y)$ and edge fold distribution $\rho_e^\alpha(x_\alpha)$,

$$J_e(x,y) = \sum_{\alpha=1}^{n}\rho_e^\alpha(x_\alpha)\delta(y_\alpha)\theta(x_\alpha). \quad (8)$$

Clearly, the distribution of the infinitesimal edge dislocations is antisymmetry, i.e., the Burgers vectors are opposite for the two aligned folds, and the total charge is zero

$$\iint J_e(x,y)dx\,dy = 0.$$

TABLE I. Parameters in the analytical expression of the γ-potential.

Shuffle-set	$\omega_0 = 0.162\,\text{eV/Å}^2$	$\eta_0 = 2.212$	$\nu_0 = 0\,\text{Å}$	$\varsigma_0 = 0.162\,\text{eV/Å}^2$
	$\omega_1 = 0.329\,\text{eV/Å}^2$	$\eta_1 = 0.766$	$\nu_1 = -0.211\,\text{Å}$	$\varsigma_1 = 0.425\,\text{eV/Å}^2$
	$\omega_2 = 0.166\,\text{eV/Å}^2$	$\eta_2 = 1.785$	$\nu_2 = -0.109\,\text{Å}$	$\varsigma_2 = 0.202\,\text{eV/Å}^2$
Glide-set	$\omega_0 = 6.48\,\text{eV/Å}^2$	$\eta_0 = 0.31$	$\nu_0 = 0\,\text{Å}$	$\varsigma_0 = 6.48\,\text{eV/Å}^2$
	$\omega_1 = 9.85\,\text{eV/Å}^2$	$\eta_1 = 0.53$	$\nu_1 = 0.88\,\text{Å}$	$\varsigma_1 = 10.1\,\text{eV/Å}^2$
	$\omega_2 = 23.8\,\text{eV/Å}^2$	$\eta_2 = 0.24$	$\nu_2 = 0.68\,\text{Å}$	$\varsigma_2 = 24.0\,\text{eV/Å}^2$

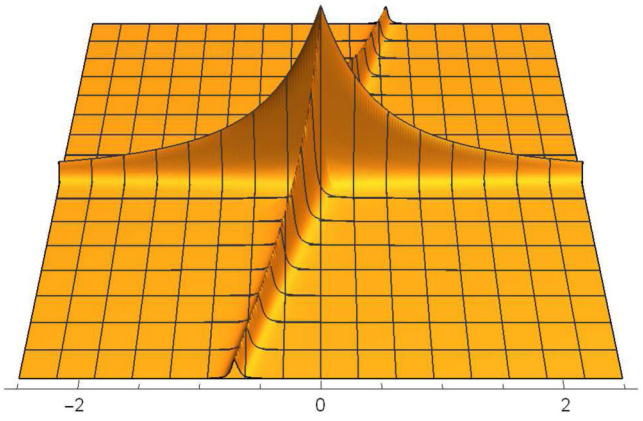

FIG. 4. Nonorthogonal fourfold core structure of $\frac{1}{2}\langle 1\bar{1}0\rangle$ screw dislocation in silicon, where the angle between neighboring folds is $\alpha = 70.53°$.

By using Eq. (4), the interaction energy of the infinitesimal edge dislocations is obtained from the superposition principle

$$U_e = -\frac{K_e}{2\pi}\int_0^{+\infty}\int_0^{+\infty}\rho_e(x)\rho_e(x')\varphi_e(x, x')dx\,dx', \tag{9}$$

where the effective interaction potential φ_e is

$$\varphi_e(x, x') = \ln\left|\frac{x - x'}{x + x'}\right|, \tag{10}$$

for the twofold structure and

$$\varphi_e(x, x') = 2\ln\left|\frac{x - x'}{x + x'}\right| + \cos\alpha\ln\left|\frac{x^2 + x'^2 - 2xx'\cos\alpha}{x^2 + x'^2 + 2xx'\cos\alpha}\right| - \frac{4xx'(x^2 + x'^2)\sin^2\alpha}{(x^2 + x'^2)^2 - 4x^2x'^2\cos^2\alpha}, \tag{11}$$

for the fourfold structure (see the Appendix).

From the fully discrete models of dislocations, which can be solved exactly, there exists contact interaction for the dislocation[52]

$$U_c = \frac{n}{4}\int_0^{\infty}(\beta_s\rho_s^2 + \beta_e\rho_e^2)dx, \quad n = 4, \tag{12}$$

where β_s and β_e are the effective force constants between atom chains on a slip plane.[24] For the edge component resulting from the spatial change, $\beta_e \approx 0$.[37]

Finally, the energy functional of a nonorthogonal fourfold screw dislocation is

$$U = U_c + U_s + U_e + 4\int_0^{\infty}\gamma(u_s, u_e)dx. \tag{13}$$

The relative slip u_s and spatial change u_e, respectively, relate to fold distributions in the following way,

$$\rho_s = \frac{du_s}{dx}, \quad \rho_e = \frac{du_e}{dx}.$$

The core structure of a perfect dislocation results from the balance between the attracting interaction and the expelling interaction. The expelling interaction is given by the dislocation interactions discussed above. The necessary attracting interaction is provided by the γ-potential.

The dislocation equation that governs the core structure is given by the variational principle

$$\frac{\delta U}{\delta u_s} = 0, \quad \frac{\delta U}{\delta u_e} = 0. \tag{14}$$

Noting that $\phi(x, x') = \phi(x', x)$, it is straightforward to find the dislocation equation to be

$$-\frac{\beta_s}{2}\frac{d^2u_s(x)}{dx^2} + \frac{K_s}{2\pi}\int_0^{+\infty}\frac{\partial\varphi_s(x, x')}{\partial x}\frac{du_s(x')}{dx'}dx' = f_s,$$
$$\frac{K_e}{2\pi}\int_0^{+\infty}\frac{\partial\varphi_e(x, x')}{\partial x}\frac{du_e(x')}{dx'}dx' = f_e, \tag{15}$$

where

$$f_s = -\frac{\partial\gamma(u_e, u_s)}{\partial u_s}, \quad f_e = -\frac{\partial\gamma(u_e, u_s)}{\partial u_e}.$$

The energy factors of the screw and edge dislocations are[1]

$$K_s = (c'_{44}c'_{55} - c'^2_{16})^{1/2}, \quad K_e = (\bar{c}'_{11} + c'_{12})\left[\frac{c'_{44}(\bar{c}'_{11} - c'_{12})}{(c'_{11} + c'_{12} + 2c'_{44})c'_{11}}\right]^{1/2} \tag{16}$$

and the effective force constant is

$$\beta_s = \frac{(c_{11} - c_{12})a_0^3}{16\sigma},$$

where c_{ij} is the elastic constant used typically and c'_{ij} is the elastic constant in the intrinsic coordinate system of the dislocation.[1]

IV. EQUILIBRIUM CORE STRUCTURES AND THEIR ENERGY

In this section, we investigate the equilibrium cores by solving the dislocation equation given in Sec. III and study the structural stability in terms of energetics. The physical constants in the left-hand side of the dislocation equation are given in Table II, where the elastic constants are $c_{11} = 154$ GPa, $c_{12} = 59$ GPa, and $c_{44} = 99$ GPa.[8]

TABLE II. The energy factors and the effective force constant.

K_s	K_e	β_s/a_0
68.57 (GPa)	95.99 (GPa)	13.71 (GPa)
0.428 (eV/Å^3)	0.599 (eV/Å^3)	0.086 (eV/Å^3)

TABLE III. The values of parameters in the approximated solutions.

	s_1	s_2	q_0	e_1	e_2	$\kappa_s b$	$\kappa_e b$
Twofold shuffle core	0.050	0.210	0	−0.054	0.012	1.283	1.320
Twofold glide core	0.690	0.18	0	0.150	0	2.631	3.500
Fourfold shuffle core	0.480	0.290	−1	−0.052	0.017	1.000	1.160
Fourfold glide core	0.890	0.200	−1	0.120	0.100	2.500	3.100

For the planar core ($n = 2$), the approximated solution is[53]

$$u_s(x) = \frac{b}{\pi}\left[\arctan q + \frac{s_1 q}{1+q^2} + \frac{s_2 q}{(1+q^2)^2}\right], \quad q = \kappa_s x,$$
$$u_e(x) = \frac{e_1 b}{1+p^2} + \frac{e_2 b}{(1+p^2)^2}, \quad p = \kappa_e x, \tag{17}$$

where s_1, s_2, e_1, e_2, κ_s, and κ_e are parameters to be determined.

For the fourfold structure ($n = 4$), the approximated solution is formally similar to Eq. (17) except a phase shift q_0,[28]

$$u_s(x) = \frac{b_1}{\pi}\left[\arctan(q-q_0) + \frac{s_1(q-q_0)}{1+(q-q_0)^2} + \frac{s_2(q-q_0)}{[1+(q-q_0)^2]^2}\right] + b_2, \quad q = \kappa_s x,$$
$$u_e(x) = \frac{e_1 b}{1+(p-q_0)^2} + \frac{e_2 b}{[1+(p-q_0)^2]^2}, \quad p = \kappa_e x, \tag{18}$$

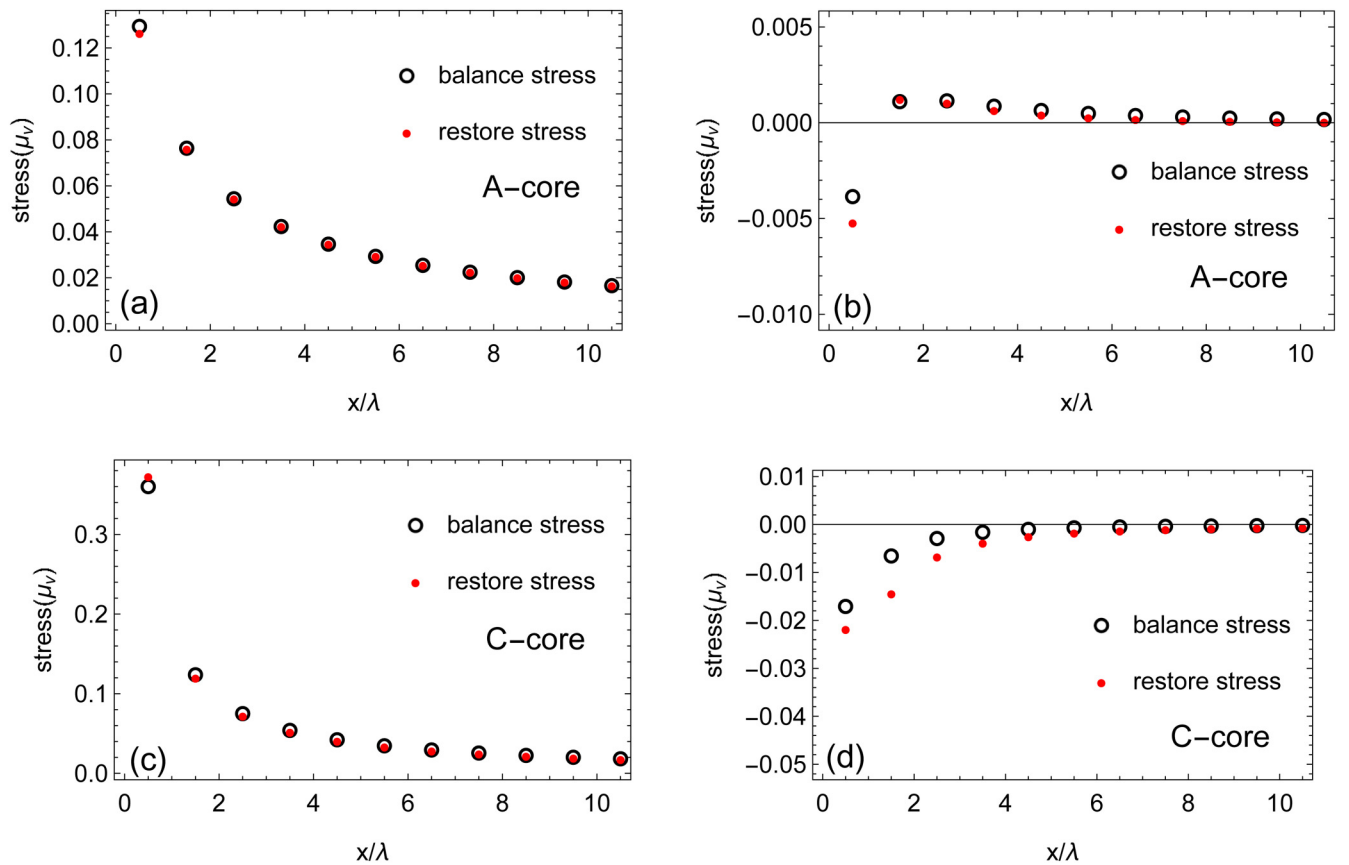

FIG. 5. For the fourfold cores, the restorative stress (solid dots) resulting from the misfit interaction (γ-potential) and the balance stress (empty circles) resulting from the infinitesimal dislocation interaction are, respectively, plotted, where $\lambda = 3.34$ Å is the distance between adjacent lattice lines parallel to the dislocation line, and the stress unit is the Reuss average shear modulus $\mu_v \approx K_s = 68.57$ GPa.[1] (a) The shear stress of the shuffle-set dislocation. (b) The normal stress of the shuffle-set dislocation. (c) The shear stress of the glide-set dislocation. (d) The normal stress of the glide-set dislocation. The figures also indicate that the approximated solutions are satisfactory.

where the new constants b_1 and b_2 are determined by the boundary conditions

$$u_s(0)=\frac{b}{4},\quad u_s(+\infty)=\frac{b}{2}. \tag{19}$$

The boundary conditions ensure that each fold has a 1/4 Burgers vector and the total Burgers vector is b. From the boundary conditions in Eq. (19), it is easy to obtain the parameters b_1 and b_2,

$$\begin{aligned}\frac{b_1}{b}&=\frac{\pi(1+q_0^2)^3}{4q_0\left[s_1(1+q_0^2)^2+s_2(1+q_0^2)\right]+2[\pi+2\tan^{-1}(q_0)](1+q_0^2)^3},\\ \frac{b_2}{b}&=\frac{4q_0\left[s_1(1+q_0^2)^2+s_2(1+q_0^2)\right]+\left[\pi+4\tan^{-1}(q_0)\right](1+q_0^2)^3}{8q_0\left[s_1(1+q_0^2)^2+s_2(1+q_0^2)\right]+4[\pi+2\tan^{-1}(q_0)](1+q_0^2)^3}.\end{aligned} \tag{20}$$

The exact solution of an orthogonal fourfold structure with $\alpha=\pi/2$ was obtained in Ref. 28. The relation between the phase

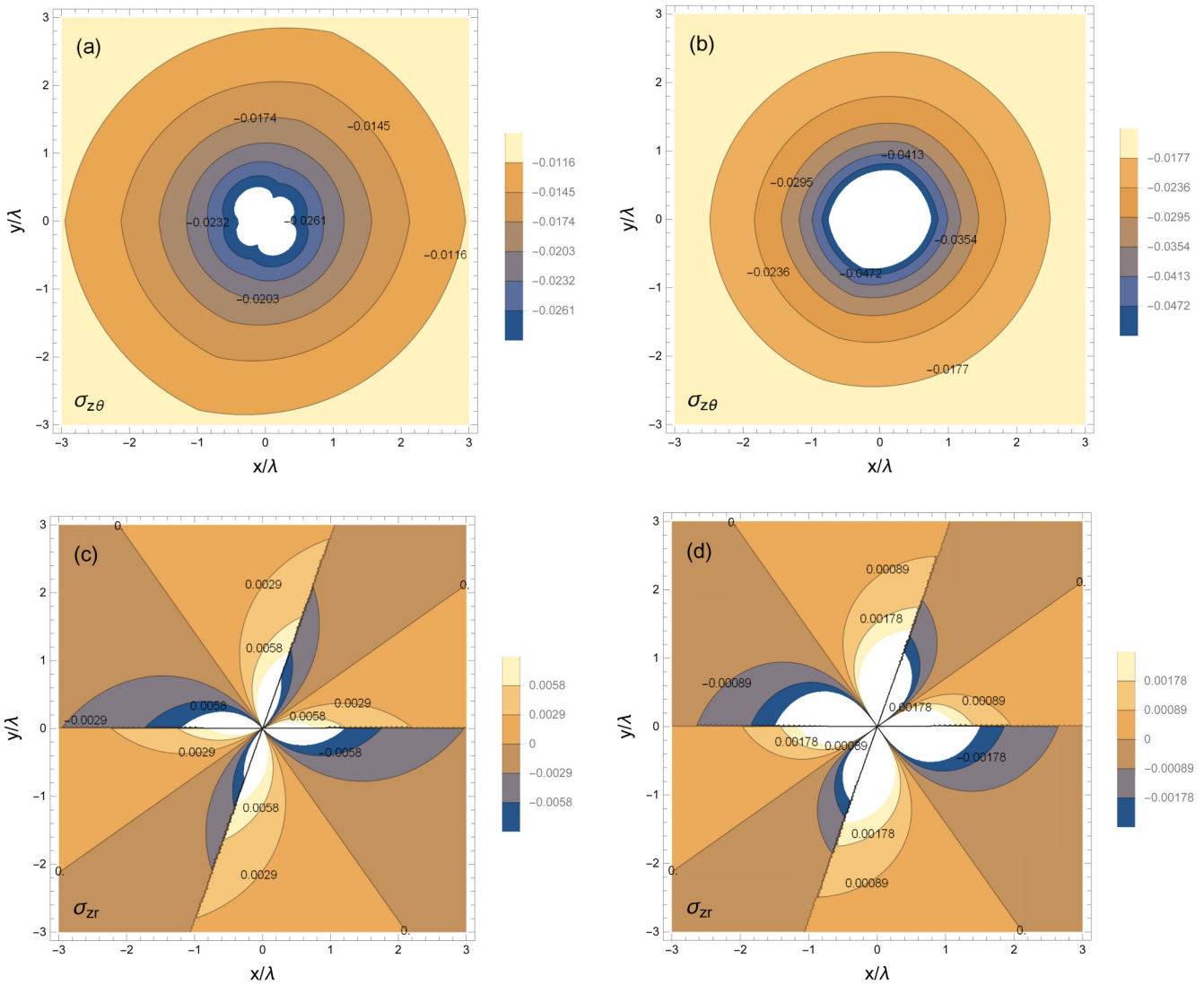

FIG. 6. Counterplot pictures of stress for fourfold structure in cylindrical coordinates. (a) and (b) represent stress fields $\sigma_{z\theta}$ of the shuffle-set and the glide-set, respectively; (c) and (d) represent the stress field σ_{zr} of the shuffle-set and the glide-set, respectively. The coordinates of ranges of scale in $[-3\lambda, 3\lambda]$, where $\lambda = 3.34$ Å is the distance between adjacent lattice lines parallel to the dislocation line, and the unit of stress is the Reuss average shear modulus $\mu_v \approx K_s = 68.57$ GPa.[1]

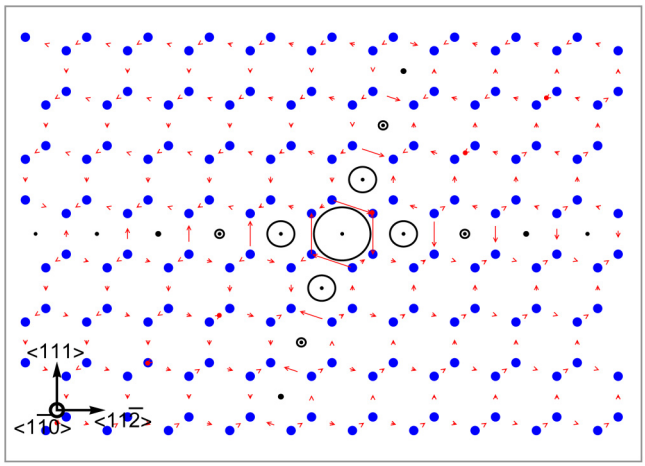

FIG. 7. The differential displacement map of the structure of fourfold shuffle dislocation. The length of the arrow is proportional to the out-of-plane $(1\bar{1}0)$ shift between neighboring atoms. The size of the circle represents the magnitude of dislocation density that distributes into the two {111} planes symmetrically.

shift q_0 and the fold number n is

$$q_0 = -\cot\frac{\pi}{n}.$$

We assume that this relation is approximately valid for this case $\alpha = 70.53^\circ \approx 90^\circ$, i.e., $q_0 \approx -1$. The parameters s_1, s_2, e_1, e_2, κ_s, and κ_e are numerically determined by the Rayleigh–Ritz variation method with expressions as in Eqs. (17) and (18) as trial solutions. The values of these parameters are listed in Table III.

Note that for the shuffle-set dislocation, parameters e_1 and e_2 are very small, and thus the spatial variation induced by the dislocation is negligible. By contrast, for the glide-set dislocation, the space is broadened remarkably by appearance of the dislocation. The spatial increases of the glide-set are as large as approximately 50.

In Fig. 5, the restore forces resulting from the γ-potential are, respectively, plotted for the fourfold A-core (shuffle-set) and C-core (glide-set). The qualitative behaviors of forces along the slip are similar. However, the magnitude of the force in the C-core is much larger than that in the A-core. The normal force of the C-core is opposite to that of the A-core because the space had been broadened for the glide-set and narrowed for the shuffle-set. Shear stress at the core is nearly the same order of elastic modulus. The normal stress is considerably smaller due to the relaxation of space. To verify the accuracy of the solution, the balance stresses resulting from infinitesimal dislocation interactions are also plotted in Fig. 5. We see that the attracting force associated with the γ-potential is approximately equal to the expelling force associated with the infinitesimal dislocation interaction, and thus the expressions in Eq. (18) are indeed the solutions of the dislocation equations.

The entire stress field of the dislocation is also evaluated using the superposition principle.[27] In Fig. 6, the counterplot of the stress field is shown for fourfold screw dislocations. It is clear that the stress of the glide-set dislocation is much stronger than that of the shuffle-set dislocation. In Fig. 7, the differential displacement map of the fourfold shuffle-set dislocation is presented, where the contribution of the edge component is neglected because the spatial variation is very small.

It is useful to study the stability of the core structures from the viewpoint of energetics. To have a definite zero-point of energy, the core energy U_{core} is extracted from the total energy U in the following way,

$$U_{core} = U - \frac{Kb^2}{4\pi}\ln\frac{R_0}{b}. \tag{21}$$

Substituting the solutions into the energy functional, we calculate the energy of the equilibrium structures of the screw dislocation. The final results are listed in Table IV. It is clear that among the equilibrium cores of the dislocation, the energy of the shuffle-set dislocation (A-core) with the fourfold core was much lower than that of the others, and the glide-set dislocation (C-core) with the planar core had the highest energy. Therefore, in energetics, the fourfold shuffle-set dislocation is the most stable and the planar glide-set dislocation is completely unstable. This result agrees with that obtained by *ab initio* calculations.[11]

For the planar core, the Peierls barrier can be obtained from the assumption of rigid dislocation.[24] In Fig. 8, the dislocation energy as a function of the dislocation position is plotted. The Peierls barrier is $E_p = 0.016\,\text{eV/Å}$ for the shuffle dislocation and is $E_p = 0.923\,\text{eV/Å}$ for the glide dislocation. From Fig. 8, we see that the phase of oscillation of the misfit energy (γ-potential) is opposite to that of the infinitesimal dislocation interaction energy. Contributions by the misfit energy and interaction energy strongly cancel each other out. If only the contribution of misfit energy was considered, the Peierls barrier would be much larger than it should. Peierls stress estimated from the barrier was $0.009\,\text{eV/Å}^3$ for the shuffle-set planar structure. This is lower than the experimental value (0.043–$0.213\,\text{eV/Å}^3$).[25] This might have been obtained because of the stability of the core structure. As we learned above, the planar core does not have the lowest energy. The critical stress observed in experiments cannot simply be identified with the Peierls stress calculated in this way. For the glide-set planar structure, the relevant Peierls stress is $0.497\,\text{eV/Å}^3$, which is much larger than that of the shuffle-set dislocation.

TABLE IV. Energies of the equilibrium structures of the $\langle 1\bar{1}0\rangle$ screw dislocation in units of eV/Å.

	U_c	U_s	U_e	U_γ	U_{core}
Twofold shuffle	0.109	−0.170	0.003	0.605	0.547
Twofold glide	0.401	0.590	0.039	0.794	1.824
Fourfold shuffle	0.034	−0.540	0.001	0.573	0.068
Fourfold glide	0.176	0.379	0.019	0.739	1.313

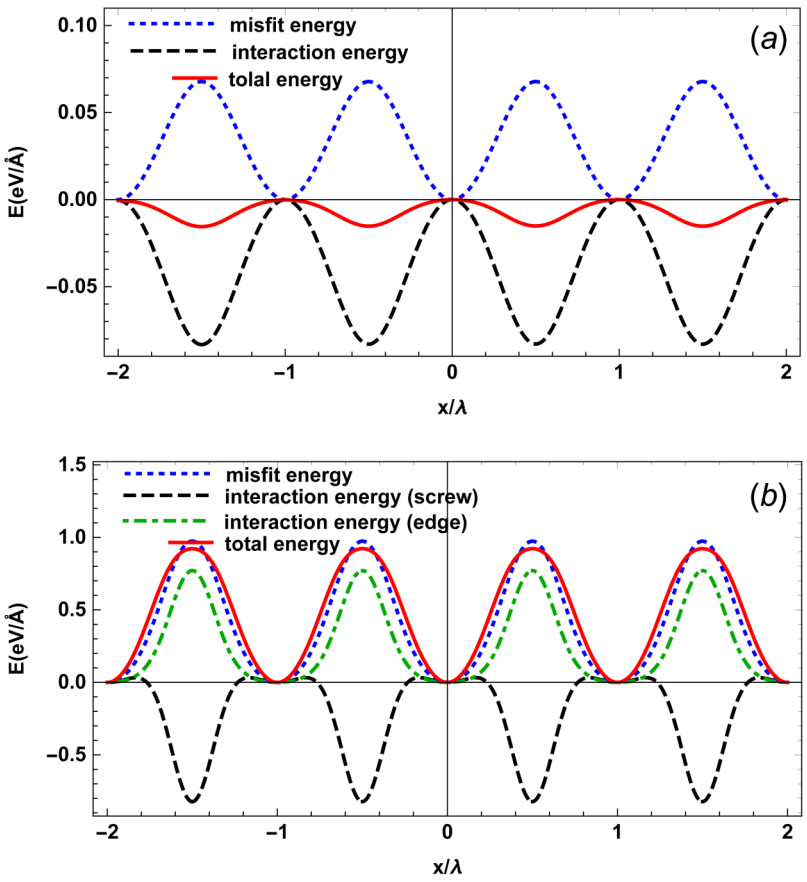

FIG. 8. The Peierls barrier in units of eV/Å for the planar structures of shuffle-set (a) and glide-set (b), and $\lambda = 3.34$ Å.

V. DISCUSSION AND SUMMARY

The $\langle 1\bar{1}0 \rangle$ screw dislocation in silicon exhibits a variety of equilibrium core structures. There are two kinds of screw dislocations: the glide-set screw dislocation and the shuffle-set screw dislocation. Because of the low stacking fault energy of the glide-set, the relevant dislocation is further classified into a dissociated dislocation and a compact (nondissociated) dislocation. For the glide-set screw dislocation, the dissociated dislocation has the lowest energy. The glide-set screw dislocation dissociates into two 30° partial dislocations separated by a ribbon of an intrinsic stacking fault. Moreover, because a screw dislocation has many slip planes, as first proposed by Hirsch, its core might distribute to a single slip plane to form a planar structure or to several slip planes to form a nonplanar structure.[26] On the other hand, as shown in Fig. 1, the $\langle 1\bar{1}0 \rangle$ screw dislocation can also be classified into A-, B-, and C-cores according to the center position of their core. Apparently, the A-core is the shuffle-set dislocation and the C-core is the glide-set dislocation. As for the B-core, it may be a shuffle-set or a glide-set dislocation owing to the shuffle-set slip plane and the glide-set slip plane cross at point B. Furthermore, the B-core may be a mixed dislocation with the core distributed to both the glide and shuffle slip planes. As mentioned above, the equilibrium core structure is not uniquely determined by its center because a screw dislocation may be planar or nonplanar.[26]

Using *ab initio* simulations, Arias and Joannopoulos produced the atomic configuration of the A-core using the bonding topology proposed by Hornstra and estimated the core energy.[19,20] Koizumi *et al.* first pointed out the significance of the B-core and proposed possible transformation between the glide-set and the shuffle-set dislocations. They calculated the core structures and their stability with the Stillinger–Weber potential for interatomic interaction and concluded that the B-core is the most stable.[9] Later, Pizzagalli *et al.* investigated the stability of the screw dislocation and found that it depends on the classical potential used. They also concluded that the A-core is the most stable core when the correct potential is used.[11] Our theoretical results agree with those obtained by Pizzagalli *et al.* From Table IV, we see that the energy (0.068 eV/Å) of the A-core with four symmetric fold is much lower than that of the C-core (1.824 eV/Å and 1.313 eV/Å for the twofold and the fourfold, respectively). The energy of the twofold A-core is 0.547 eV/Å higher than that of the fourfold A-core. From the Peierls periodic potential shown in Fig. 8, we know that the energy of the twofold B-core is slightly lower than that of the twofold A-core, but remarkably higher than that of the fourfold A-core. Unfortunately, the energy of the fourfold B-core is not

calculated because the two crossed slip planes involved are not equivalent. Clearly, inequivalent slip planes imply an asymmetric multifold core. Although the theory used here can be generalized to treat asymmetric multifold cores, the quantitative study of an asymmetric multifold core is too complex to be presented. However, even though the detailed structure and exact energy of the fourfold B-core have not been calculated, we can still conclude that its energy is larger than that of the A-core on the basis of physical interpretation.

If a dislocation is viewed as a condensate composed of infinitesimal dislocations, the equilibrium core structure results from the balance between the attracting interaction and the expelling interaction. The expelling interaction is provided by dislocation interactions and the attracting interaction by the γ-potential. It has been proven that in the Peierls theory, energy associated with the γ-potential is almost constant if the equilibrium equation is satisfied.[54] That is to say, the attracting energy is almost independent of the configuration of the equilibrium core. As a result, the dislocation energy is mainly dominated by the expelling interaction. Because the expelling interaction always renders the constituents far from one another, a wider dislocation core has lower energy. On the contrary, it is well known that the width of the dislocation core is mainly determined by the height of the unstable stacking energy (the maximum of the γ-potential). The higher the unstable stacking energy, the narrower the dislocation. Therefore, the dislocation has relatively high energy if its γ-potential has a large unstable stacking energy. For the screw dislocation in silicon, the unstable stacking energy of the glide-set is much larger than that of the shuffle-set. Thus, we can physically explain why the fourfold A-core has the lowest energy. From this expelling interaction-dominating rule, we can also qualitatively conclude that in terms of energy, the B-core is smaller than the C-core and larger than the A-core.

In summary, based on the concept of infinitesimal dislocation, the energy functional and equilibrium equation for the $\langle 1\bar{1}0\rangle$ screw dislocation in silicon are successfully obtained in the frame of the Peierls theory. Combined with the γ-potential calculated using *ab initio*, the fundamental equation is used to investigate to the core structures and related energy of the $\langle 1\bar{1}0\rangle$ screw dislocation in silicon. It is found that of the equilibrium cores of the dislocations, energy of the shuffle-set dislocation (A-core) with a fourfold core is much lower than that of the others, and the glide-set dislocation (C-core) with the planar core has the highest energy. Therefore, in energetics the fourfold shuffle-set dislocation is the most stable one and the planar glide-set dislocation is completely unstable. This result agrees with that obtained by *ab initio* calculations.[11] A displacement difference map and the stress field of the $\langle 1\bar{1}0\rangle$ screw dislocation are also presented for the most stable A-core. The dislocations might have reconstructed their cores due to the appearance of dangling bonds.[21] The problem of core reconstruction cannot be dealt with in the frame of the Peierls theory. We hope that the theory can be improved to address core reconstruction in the future.

ACKNOWLEDGMENTS

This work is supported by the National Natural Science Foundation of China (NNSFC, Grant No. 11874093).

APPENDIX: INTERACTION ENERGY FUNCTIONAL IN TERMS OF INFINITESIMAL DISLOCATION DISTRIBUTION

The energy of interaction per unit length between parallel dislocations is given by[1]

$$\frac{W_{12}}{L} = -\frac{K_s}{2\pi}(\boldsymbol{b_1}\cdot\boldsymbol{\xi})(\boldsymbol{b_2}\cdot\boldsymbol{\xi})\ln\frac{R}{R_0} - \frac{K_e}{2\pi}[(\boldsymbol{b_1}\times\boldsymbol{\xi})\cdot(\boldsymbol{b_2}\times\boldsymbol{\xi})]\ln\frac{R}{R_0} - \frac{K_e}{2\pi R^2}[(\boldsymbol{b_1}\times\boldsymbol{\xi})\cdot\boldsymbol{R}][(\boldsymbol{b_2}\times\boldsymbol{\xi})\cdot\boldsymbol{R}]. \tag{A1}$$

The first term in Eq. (A1) describes the interaction between the screw components, and the last two terms describe the interaction between edge components:

1. Screw component

For the screw component, the last two terms in Eq. (A1) vanish. The interaction energy for infinitesimal screw dislocations in a single fold is

$$U_{11} = \frac{1}{2}\int_0^{+\infty}\int_0^{+\infty} -\frac{K_s}{2\pi}\rho_s(x)\rho_s(x')\ln\frac{|x-x'|}{R_0}\,dx\,dx', \tag{A2}$$

where factor $1/2$ comes from double counting.

The interaction energy of infinitesimal screw dislocations in two folds is

$$U_{12} = \int_0^{+\infty}\int_0^{+\infty} -\frac{K_s}{2\pi}\rho_s(x)\rho_s(x')\ln\frac{\sqrt{x^2+x'^2-2xx'\cos\alpha}}{R_0}\,dx\,dx', \tag{A3}$$

where $R = \sqrt{x^2+x'^2-2xx'\cos\alpha}$, α is the angle two folds. Noting that the angle between fold 2 and fold 3 in Fig. 9 is $\alpha \to \pi - \alpha$, the interaction energy is

$$U_{23} = \int_0^{+\infty}\int_0^{+\infty} -\frac{K_s}{2\pi}\rho_s(x)\rho_s(x')\ln\frac{\sqrt{x^2+x'^2+2xx'\cos\alpha}}{R_0}\,dx\,dx' \tag{A4}$$

and that between fold 1 and fold 3 in Fig. 9 is $\alpha \to \pi$. The interaction energy is

$$U_{13} = \int_0^{+\infty}\int_0^{+\infty} -\frac{K_s}{2\pi}\rho_s(x)\rho_s(x')\ln\frac{|x+x'|}{R_0}\,dx\,dx'. \tag{A5}$$

The total interaction energy of the screw component is

$$U_s = 4U_{11} + 2U_{12} + 2U_{23} + 2U_{13} = -\frac{K_s}{2\pi}\int_0^{+\infty}\int_0^{+\infty}\rho_s(x)\rho_s(x')\varphi_s(x,x')dx\,dx', \tag{A6}$$

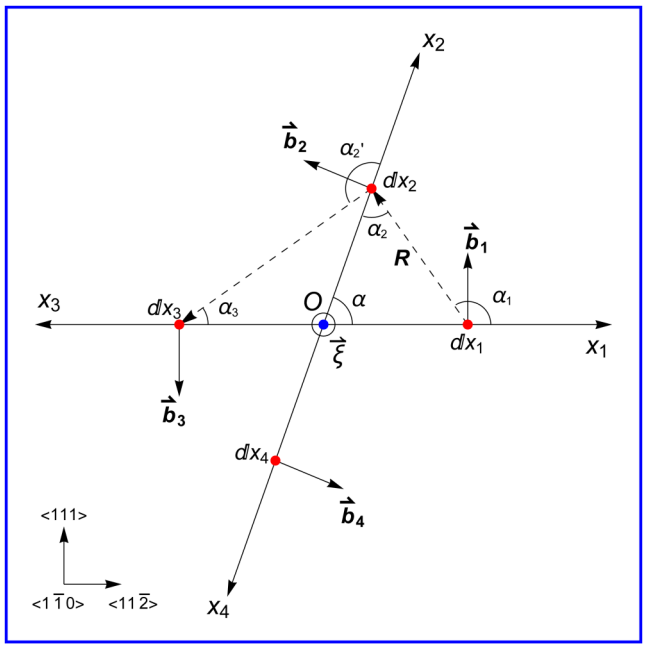

FIG. 9. The coordinates of the fourfold structure. $\vec{\xi}$ is the dislocation line perpendicular to the paper plane and its direction is outward, α is the angle between the two slip planes, and $\cos\alpha = 1/3$. $X_i (i = 1, 2, 3, 4)$ is the coordinate of the slip plane, assuming that each slip plane is equal. $b_i (i = 1, 2, 3, 4)$ is the edge component perpendicular to the slip plane, and R is the separation between infinitesimal dislocation distributions.

where

$$\varphi_s(x, x') = 2\ln\frac{|x^2 - x'^2|}{R_0^2} + \ln\frac{|x^4 + x'^4 - 2x^2x'^2\cos 2\alpha|}{R_0^4}. \quad \text{(A7)}$$

2. First item of edge component

For the edge component, the value of the first term in Eq. (A1) vanishes. As shown in Fig. 9, the interaction energy of the infinitesimal edge dislocation in a single fold from the second term in Eq. (A1) is given by

$$U_{11} = \frac{1}{2}\int_0^{+\infty}\int_0^{+\infty} -\frac{K_e}{2\pi}\rho_e(x)\rho_e(x')\ln\frac{|x - x'|}{R_0}dx\,dx', \quad \text{(A8)}$$

where factor $1/2$ comes from double counting.

The interaction energy for the infinitesimal edge dislocations in two folds from the second term in Eq. (A1) is given by

$$U_{12} = \cos\alpha\int_0^{+\infty}\int_0^{+\infty} -\frac{K_e}{2\pi}\rho_e(x)\rho_e(x')\ln\frac{\sqrt{x^2 + x'^2 - 2xx'\cos\alpha}}{R_0}dx\,dx', \quad \text{(A9)}$$

where $R = \sqrt{x^2 + x'^2 - 2xx'\cos\alpha}$, α is the angle between folds, and the factor $\cos\alpha$ comes from the fact that there is an angle between the directions following the calculation of the crossproduct of each infinitesimal edge dislocation and dislocation line. Noting that the angle between fold 2 and fold 3 in Fig. 9 is $\alpha \to \pi - \alpha$, the interaction energy is

$$U_{23} = \cos(\pi - \alpha)\int_0^{+\infty}\int_0^{+\infty} -\frac{K_e}{2\pi}\rho_e(x)\rho_e(x')\ln\frac{\sqrt{x^2 + x'^2 + 2xx'\cos\alpha}}{R_0}dx\,dx'\,dx\,dx' \quad \text{(A10)}$$

and given that the angle between folds 1 and 3 in Fig. 9 is $\alpha \to \pi$, the interaction energy from the second term in Eq. (A1) is

$$U_{13} = \int_0^{+\infty}\int_0^{+\infty}\frac{K_e}{2\pi}\rho_e(x)\rho_e(x')\ln\frac{|x + x'|}{R_0}dx\,dx'. \quad \text{(A11)}$$

The total energy of the edge component from the second term in Eq. (A1) for the fourfold structure is

$$\begin{aligned} U_e^{(1)} &= 4U_{11} + 2U_{12} + 2U_{23} + 2U_{13} \\ &= -\frac{K_e}{2\pi}\int_0^{+\infty}\int_0^{+\infty}\rho_e(x)\rho_e(x')\varphi_e^{(1)}(x, x')dx\,dx', \end{aligned} \quad \text{(A12)}$$

where

$$\varphi_e^{(1)}(x, x') = 2\ln\left|\frac{x - x'}{x + x'}\right| + \cos\alpha\ln\left|\frac{x^2 + x'^2 - 2\cos\alpha xx'}{x^2 + x'^2 + 2\cos\alpha xx'}\right|. \quad \text{(A13)}$$

3. Second item of edge component

As shown in Fig. 9, for each fold structure, the interaction energy of infinitesimal screw dislocations in a single fold from the third term (i.e., the second edge component) in Eq. (A1) is given by

$$U_{11} = \frac{1}{2}\int_0^{+\infty}\int_0^{+\infty} -\frac{K_e}{2\pi}\rho_e(x)\rho_e(x')dx\,dx', \quad \text{(A14)}$$

where factor $1/2$ comes from double counting.

The interaction energy for infinitesimal edge dislocations in two folds from the third term in Eq. (A1) is given by

$$U_{12} = \int_0^{\infty}\int_0^{\infty} -\frac{K_e}{2\pi}\rho_e(x)\cos\alpha_1\rho_e(x')\cos\alpha_2\,dx\,dx'. \quad \text{(A15)}$$

The angles α_1 and α_2 are shown in Fig. 9 and

$$\cos\alpha_1 = -\frac{x^2 + R^2 - x'^2}{2xR}, \quad \cos\alpha_2 = \frac{x'^2 + R^2 - x^2}{2x'R}, \quad \text{(A16)}$$

where

$$R = \sqrt{x^2 + x'^2 - 2xx'\cos\alpha} \quad \text{(A17)}$$

is the distance between the infinitesimal edge dislocations of fold 1 and fold 2.

As with U_{12}, the interaction energy between fold 2 and fold 3 in Fig. 9 is given by

$$U_{23} = \int_0^{\infty}\int_0^{\infty} -\frac{K_e}{2\pi}\rho_e(x)\cos\alpha_2'\rho_e(x')\cos\alpha_3\,dx\,dx'. \tag{A18}$$

The angles α_2' and α_3 are shown in Fig. 9, and

$$\cos\alpha_2' = -\frac{x^2+R^2-x'^2}{2xR}, \quad \cos\alpha_3 = \frac{x'^2+R^2-x^2}{2x'R}, \tag{A19}$$

where the angle between fold 2 and fold 3 is $\pi-\alpha$. Thus, the distance between their infinitesimal edge dislocations is

$$R = \sqrt{x^2+x'^2+2xx'\cos\alpha}. \tag{A20}$$

Between fold 1 and fold 3, as shown in Fig. 9, the interaction energy from the third term in Eq. (A1) is given by

$$U_{13} = \int_0^{+\infty}\int_0^{+\infty}\frac{K_e}{2\pi}\rho_e(x)\rho_e(x')dx\,dx'. \tag{A21}$$

The total energy of the edge component from the third term in Eq. (A1) for the fourfold structure is

$$\begin{aligned} U_e^{(2)} &= 4U_{11}+2U_{12}+2U_{23}+2U_{13} \\ &= -\frac{K_e}{2\pi}\int_0^{\infty}\int_0^{\infty}\rho(x)\rho(x')\varphi_e^{(2)}(x,x')dx\,dx', \end{aligned} \tag{A22}$$

where

$$\begin{aligned} \varphi_e^{(2)}(x,x') &= 2\cos\alpha_1\cos\alpha_2+2\cos\alpha_2'\cos\alpha_3 \\ &= -\frac{4xx'(x^2+x'^2)\sin^2\alpha}{(x^2+x'^2)^2-4x^2x'^2\cos^2\alpha}. \end{aligned} \tag{A23}$$

According to Eqs. (A13) and (A23), we can obtain

$$\begin{aligned} \varphi_e(x,x') = {} & 2\ln\left|\frac{x-x'}{x+x'}\right|+\cos\alpha\ln\left|\frac{x^2+x'^2-2xx'\cos\alpha}{x^2+x'^2+2xx'\cos\alpha}\right| \\ & -\frac{4xx'(x^2+x'^2)\sin^2\alpha}{(x^2+x'^2)^2-4x^2x'^2\cos^2\alpha}. \end{aligned} \tag{A24}$$

REFERENCES

[1]J. P. Hirth and J. Lothe, *Theory of Dislocations*, 2nd ed. (Wiley, New York, 1982).

[2]W. Cai, V. V. Bulatov, J. Chang, J. Li, and S. Yip, "Dislocation core effects on mobility," in *Dislocations in Solids*, edited by F.R.N. Nabarro and J.P. Hirth, (Elsevier, 2004), Chap. 64, Vol. 12, p. 1.

[3]J. R. Chelikowsky and J. C. H. Spence, "Line defects in silicon: The 90° partial dislocation," Phys. Rev. B **30**(2), 694–701 (1984).

[4]J. Bennetto, R. W. Nunes, and D. Vanderbilt, "Structure, barriers, and relaxation mechanisms of kinks in the 90° partial dislocation in silicon," Phys. Rev. Lett. **77** (8), 1516–1519 (1996).

[5]J. Bennetto, R. W. Nunes, and D. Vanderbilt, "Period-doubled structure for the 90° partial dislocation in silicon," Phys. Rev. Lett. **79**(2), 245–248 (1997).

[6]A. Valladares, J. A. White, and A. P. Sutton, "First principles simulations of the structure, formation, and migration energies of kinks on the 90° partial dislocation in silicon," Phys. Rev. Lett. **81**, 4903–4906 (1998).

[7]N. Oyama and T. Ohno, "Migration processes of the 30° partial dislocation in silicon," Phys. Rev. Lett. **93**(19), 195502 (2004).

[8]S. Wang, L. Huang, and R. Wang, "The 90° partial dislocation in semiconductor silicon: An investigation from the lattice P-N theory and the first principle calculation," Acta Mater. **109**, 187–201 (2016).

[9]H. Koizumi, Y. Kamimura, and T. Suzuki, "Core structure of a screw dislocation in a diamond-like structure," Philos. Mag. A **80**(3), 609–620 (2000).

[10]M. Miyata and T. Fujiwara, "Ab initio calculation of Peierls stress in silicon," Phys. Rev. B **63**(4), 045206 (2001).

[11]L. Pizzagalli, P. Beauchamp, and J. Rabier, "Undissociated screw dislocations in silicon: Calculations of core structure and energy," Philos. Mag. **83**(10), 1191–1204 (2003).

[12]L. Pizzagalli and P. Beauchamp, "First principles determination of the Peierls stress of the shuffle screw dislocation in silicon," Philos. Mag. Lett. **84**(11), 729–736 (2004).

[13]L. Pizzagalli, J. L. Demenet, and J. Rabier, "Theoretical study of pressure effect on the dislocation core properties in semiconductors," Phys. Rev. B **79**(4), 045203 (2009).

[14]Z. Li and R. C. Picu, "Shuffle-glide dislocation transformation in Si," J. Appl. Phys. **113**(8), 083519 (2013).

[15]H. Zhang, C. Zhang, C. Zeng, and L. Tong, "The properties of shuffle screw dislocations in semiconductors silicon and germanium," Open Mater. Sci. J. **9**, 10–13 (2015).

[16]L. Pizzagalli, A. Pedersen, A. Arnaldsson, H. Jónsson, and P. Beauchamp, "Theoretical study of kinks on screw dislocation in silicon," Phys. Rev. B **77**, 064106 (2008).

[17]K. Wessel and H. Alexander, "On the mobility of partial dislocations in silicon," Philos. Mag. **35**(6), 1523–1536 (1977).

[18]J. Rabier, P. Cordier, T. Tondellie, J. L. Demenet, and H. Garem, "Dislocation microstructures in Si plastically deformed at RT," J. Phys. Condens. Matter **12**, 10059–10064 (2000).

[19]J. Hornstra, "Dislocations in the diamond lattice," J. Phys. Chem. Solids **5**, 129–141 (1958).

[20]T. A. Arias and J. D. Joannopoulos, "Ab initio theory of dislocation interactions: From close-range spontaneous annihilation to the long-range continuum limit," Phys. Rev. Lett. **73**(5), 680–683 (1994).

[21]K.-M. Ho, C.-Z. Wang, J. Li, and S. Yip, "Undissociated screw dislocation in Si: Glide or shuffle set?," Appl. Phys. Lett. **89**(5), 051910 (2006).

[22]L. Pizzagalli, "Atomistic modeling of the dissociation of a screw dislocation in silicon," J. Mater. Sci. **51**(6), 2869–2876 (2015).

[23]B. Joós, Q. Ren, and M. S. Duesbery, "Peierls-Nabarro model of dislocations in silicon with generalized stacking-fault restoring forces," Phys. Rev. B **50**(9), 5890–5898 (1994).

[24]S. Wang, H. Zhang, X. Wu, and R. Liu, "Theoretical calculation of the dislocation width and Peierls barrier and stress for semiconductor silicon," J. Phys. Condens. Matter **22**(5), 055801 (2010).

[25]T. Suzuki and S. Takeuchi, "Lattice defects in ceramics," in *JJAP Series*, edited by S. Takeuchi and T. Suzuki (Publ. Off. of Jpn. J. Appl. Phys., No. 2, Tokyo, 1989), p. 9.

[26]P. B. Hirsch, A. Howie, and M. J. Whelan, "A kinematical theory of diffraction contrast of electron transmission microscope images of dislocations and other defects," Phil. Trans. R. Soc. Lond. A **252**(1017), 499–529 (1960).

[27]X. Hu and S. Wang, "Nonplanar core structure of the screw dislocations in tantalum from the improved Peierls–Nabarro theory," Philos. Mag. **98**(6), 484–516 (2017).

[28]S. Wang and X. Hu, "Exact solution of the generalized Peierls equation for arbitrary n-fold screw dislocation," J. Mech. Phys. Solids **114**, 75–83 (2018).
[29]V. Vítek, "Intrinsic stacking faults in body-centred cubic crystals," Philos. Mag. **18**(154), 773–786 (1968).
[30]E. Kaxiras and M. S. Duesbery, "Free energies of generalized stacking faults in Si and implications for the brittle-ductile transition," Phys. Rev. Lett. **70**(24), 3752–3755 (1993).
[31]S.-F. Wang, X.-Z. Wu, and Y.-F. Wang, "Variational principle for the dislocation equation in lattice theory," Phys. Scr. **76**(5), 593–596 (2007).
[32]S. Wang, R. Liu, and X. Wu, "The discrete correction of the core structure for the ⟨100⟩{010} edge dislocation in bcc Fe," J. Phys. Condens. Matter **20**(48), 485207 (2008).
[33]W. Xiaozhi, W. Shaofeng, and Z. Huili, "The dissociated properties of dislocation in two-dimensional triangular lattice," Open Phys. **6**(3), 440–444 (2008).
[34]R. Wang, S. F. Wang, X. Z. Wu, and Q. Y. Wei, "First-principles determination of dislocation properties in magnesium based on the improved Peierls–Nabarro equation," Phys. Scr. **81**(6), 065601 (2010).
[35]H. Zhang, S. Wang, R. Wang, and J. Jiao, "The dislocations in graphene with the correction from lattice effect," Eur. Phys. J. B **73**(4), 489–493 (2010).
[36]X.-Z. Wu, R. Wang, S.-F. Wang, and Q.-Y. Wei, "Ab initio calculations of generalized-stacking-fault energy surfaces and surface energies for FCC metals," Appl. Surf. Sci. **256**(21), 6345–6349 (2010).
[37]S. Wang, "The dislocation equation as a generalization of Peierls equation," Philos. Mag. **95**(33), 3768–3784 (2015).
[38]S. Wang and R. Wang, "The core structure and pseudo-magnetic field of the dislocation in graphene," Europhys. Lett. **104**(2), 26002 (2013).
[39]G. Kresse and D. Joubert, "From ultrasoft pseudopotentials to the projector augmented-wave method," Phys. Rev. B **59**(3), 1758–1775 (1998).
[40]P. E. Blöchl, "Projector augmented-wave method," Phys. Rev. B **50**(24), 17953–17979 (1994).
[41]J. P. Perdew, K. Burke, and M. Ernzerhof, "Generalized gradient approximation made simple," Phys. Rev. Lett. **77**(18), 3865–3868 (1996).
[42]J. P. Perdew, K. Burke, and M. Ernzerhof, "Generalized gradient approximation made simple," Phys. Rev. Lett. **78**(18), 1396 (1996).
[43]S. F. Wang and R. Wang, "The core structure and pseudo-magnetic field of the dislocation in graphene," Europhys. Lett. **104**(2), 26002 (2013).
[44]P. B. Hirsch and M. J. Whelan, "A kinematical theory of diffraction contrast of electron transmission microscope images of dislocations and other defects," Phil. Trans. R. Soc. Lond. A **252**(1017), 499–529 (1960).
[45]W. Sigle, "High-resolution electron microscopy and molecular dynamics study of the (a/2)[111] screw dislocation in molybdenum," Philos. Mag. A **79**(5), 1009–1020 (1999).
[46]B. G. Mendis, Y. Mishin, C. S. Hartley, and K. J. Hemker, "Use of the nye tensor in analyzing HREM images of BCC screw dislocations," Philos. Mag. **86** (29–31), 4607–4640 (2006).
[47]P. D. Nellist, H. Yang, J. G. Lozano, T. J. Pennycook, and P. B. Hirsch, "Stem optical sectioning for imaging screw displacements in dislocation core structures," Microsc. Microanal. **20**(S3), 86–87 (2014).
[48]C. Woodward and S. I. Rao, "Ab-initio simulation of isolated screw dislocations in BCC MO and TA," Philos. Mag. A **81**(5), 1305–1316 (2001).
[49]J. L. Bassani, K. Ito, and V. Vitek, "Complex macroscopic plastic flow arising from non-planar dislocation core structures," Mater. Sci. Eng. A **319**, 97–101 (2001).
[50]G. Wang, A. Strachan, T. Cagin, and W. A. Goddard, "Molecular dynamics simulations of $1/2a\langle 111\rangle$ screw dislocation in TA," Mater. Sci. Eng. A **309**, 133–137 (2001).
[51]J. L. Bassani and V. Racherla, "From non-planar dislocation cores to non-associated plasticity and strain bursts," Prog. Mater. Sci. **56**(6), 852–863 (2011).
[52]W. Shaofeng, "An improvement of the Peierls equation by taking into account the lattice effects," Chin. Phys. Soc. **14**, 2575–2584 (2005).
[53]S. Wang, "Dislocation solution in slowly varying approximation," Phys. Lett. A **313**(5–6), 408–411 (2003).
[54]A. H. W. Ngan, "A generalized Peierls–Nabarro model for nonplanar screw dislocation cores," J. Mech. Phys. Solids **45**(6), 903–921 (1997).